

Mechanistic Study of Stepwise Methylisocyanide Coupling and C–H Activation Mediated by a Low-Valent Main Group Molecule

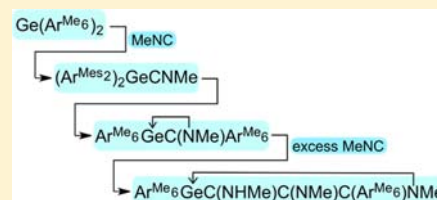
Zachary D. Brown,[†] Petra Vasko,[‡] Jeremy D. Erickson,[†] James C. Fettinger,[†] Heikki M. Tuononen,^{*,‡} and Philip P. Power^{*,†}

[†]Department of Chemistry, University of California, 1 Shields Avenue, Davis, California 95616, United States

[‡]Department of Chemistry, University of Jyväskylä, P.O. Box 35, FI-40014 Jyväskylä, Finland

Supporting Information

ABSTRACT: An experimental and DFT investigation of the mechanism of the coupling of methylisocyanide and C–H activation mediated by the germylene (germanediyl) $\text{Ge}(\text{Ar}^{\text{Me}_6})_2$ ($\text{Ar}^{\text{Me}_6} = \text{C}_6\text{H}_3-2,6(\text{C}_6\text{H}_2-2,4,6-\text{Me}_3)_2$) showed that it proceeded by initial MeNC adduct formation followed by an isomerization involving the migratory insertion of the MeNC carbon into the $\text{Ge}-\text{C}$ ligand bond. Addition of excess MeNC led to sequential insertions of two further MeNC molecules into the $\text{Ge}-\text{C}$ bond. The insertion of the third MeNC leads to methylisocyanide methyl group C–H activation to afford an azagermacyclopentadienyl species. The X-ray crystal structures of the 1:1 $(\text{Ar}^{\text{Me}_6})_2\text{GeCNMe}$ adduct, the first and final insertion products $(\text{Ar}^{\text{Me}_6})\text{GeC}(\text{NMe})\text{Ar}^{\text{Me}_6}$ and $(\text{Ar}^{\text{Me}_6})\text{GeC}(\text{NHMe})\text{C}(\text{NMe})\text{C}(\text{Ar}^{\text{Me}_6})\text{NMe}$ were obtained. The DFT calculations on the reaction pathways represent the first detailed mechanistic study of isocyanide oligomerization by a p-block element species.

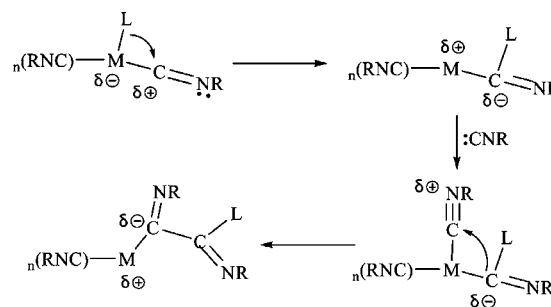


INTRODUCTION

The metal-mediated coupling and polymerization of unsaturated organic molecules are important industrial processes, and the polymers obtained are of great practical importance.^{1–4} In particular, the synthesis of heterocycles resulting from coupling and cycloaddition reactions of isocyanides with other hetero-element unsaturated species is a widely used technique.⁵ Groundbreaking work by Passerini⁶ and Ugi^{7–9} led to a dramatic expansion of the study of cyanide and isocyanide coupling chemistry, most notably their metal catalyzed oligomerization and polymerization reactions.^{10–12} However, knowledge of their mechanistic details remains limited. Some of the earliest coupling reactions were shown to be mediated by Grignard reagents¹³ and other main group metal halides,^{14,15} but most of the work on the mechanism of catalytic coupling of isocyanides has involved transition-metal complexes either of the group 10 noble metals or various first row transition-metal complexes.^{16,17}

Yamamoto and co-workers first recognized that cobalt and nickel complexes displayed high catalytic activity toward isocyanides.¹⁶ Nolte and Drenth examined the mechanism of the coupling reactions and concluded that the Lewis-acidic character of the metal center is essential to the propagation of polymerization (Scheme 1).¹⁷ The expansion of the catalytic work to the main group elements was first realized for the electropositive metals of groups 1 and 2.^{18–20} Isocyanide coordination to alkali metal cations, followed by nucleophilic attack of alkyl or amido groups, was reported by Walborsky and Lappert to form lithioaldimine¹⁸ and β -diketiminato^{19,20} complexes respectively. Subsequent coupling and migratory insertion reactions of isocyanides into metal–ligand and metal–metal bonds of main

Scheme 1. Transition-Metal Mediated Coupling of Isocyanides



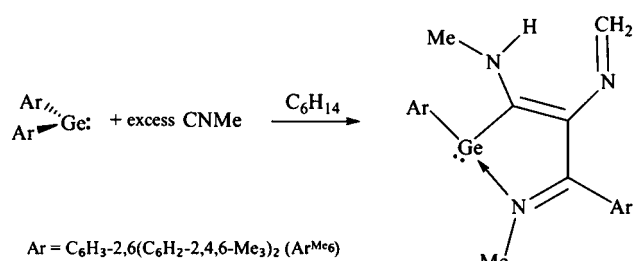
group complexes have been reported, but mechanistic information on these reactions is scarce.^{21–26}

Recently, we reported the synthesis of the adduct $(\text{Ar}^{\text{Me}_6})_2\text{GeCNBu}^t$, which underwent isobutene elimination under mild conditions to give the hydride/cyanide $(\text{Ar}^{\text{Me}_6})_2\text{Ge}(\text{H})\text{CN}$.²⁷ We now report the isolation and structural characterization of a series of compounds arising from the insertion reactions of the simplest isocyanide, MeNC , with the germylene $\text{Ge}(\text{Ar}^{\text{Me}_6})_2$ ($\text{Ar}^{\text{Me}_6} = \text{C}_6\text{H}_3-2,6(\text{C}_6\text{H}_2-2,4,6-\text{Me}_3)_2$)²⁸ and supply details of the mechanism of the subsequent transformation. We show that the simple adduct $(\text{Ar}^{\text{Me}_6})_2\text{GeCNMe}$ (**1**) is formed in the first instance, whereupon the coordinated methylisocyanide molecule in **1** then undergoes a spontaneous migratory insertion into one of the $\text{Ge}-\text{C}(\text{Ar})$ bonds to form the structural isomer $(\text{Ar}^{\text{Me}_6})\text{Ge}(\mu-\text{CNMe})(\text{Ar}^{\text{Me}_6})$ (**1'**).

Received: January 31, 2013

Published: March 11, 2013

Scheme 2. Formation of 3'' via Migratory Insertion of Methylisocyanide



If the germylene is treated with excess isocyanide, two additional molecules of methylisocyanide are incorporated into 1' to form (Ar^{Me₆})₂GeC(NHMe)C(NCH₂)C(Ar^{Me₆})NMe, (3'') (Scheme 2) via a two-fold insertion intermediate. The isolation of intermediates 1, 1', and the final product 3'' coupled with a detailed computational study of the mechanism by density functional theory (DFT) provide new insights on the migratory insertion and oligomerization reactions of isocyanides with main group complexes.

EXPERIMENTAL SECTION

General Experimental Procedures. All manipulations were carried out by using Schlenk techniques under an atmosphere of N₂. All solvents were distilled from NaK and degassed prior to use. Ge(Ar^{Me₆})₂ and Sn(Ar^{Me₆})₂ were prepared according to literature procedures.²⁸ Methylisocyanide was prepared by literature methods and stored as a 1 M solution in hexane.²⁹ ¹H NMR spectra were obtained on Varian Inova 400 and 600 MHz spectrometers and referenced to the residual protons in the solvent. Melting points were measured in glass capillaries sealed under N₂ by using a Mel-Temp II apparatus and are uncorrected. Infrared spectra were recorded using attenuated total reflectance (ATR) on a Bruker Tensor-27 infrared spectrometer. Variable temperature UV–vis data were recorded on a Cary 300 Scan spectrometer attached to a Cary Temperature Controller.

(Ar^{Me₆})₂GeCNMe (1). Method A: Methylisocyanide (1.5 mmol) was added to a stirred slurry of Ge(Ar^{Me₆})₂ (0.35 g, 0.5 mmol) in hexane (15 mL) at room temperature. The solution was allowed to stir until all the solids had dissolved and the purple color of the solution had faded to a homogeneous yellow (~15 min). The reaction mixture was stored overnight at ~7 °C to yield yellow crystals of 1 suitable for X-ray diffraction studies. If allowed to stand at ~7 °C for more than 3 days, the color of the solution changed to deep red to yield mixtures of 1 and 3''. Method B: Methylisocyanide (2 mmol) was added to a stirred slurry of Ge(Ar^{Me₆})₂ (0.35 g, 0.5 mmol) in pentane (30 mL) at room temperature. The color of the solution became yellow immediately. All volatile materials were immediately removed to afford 1 as a yellow powder in quantitative yield. Method A yield: 60% (0.22 g). Mp: 186 °C (red oil). Due to high fluxionality, ¹H and ¹³C NMR spectra could not be obtained even with cooling to –50 °C. λ_{max} (ε): 297 nm. IR (ATR) ν(C–N): 2161 cm^{–1} (m).

(Ar^{Me₆})₂Ge(CNMe)(Ar^{Me₆}) (1'). To a stirred slurry of Ge(Ar^{Me₆})₂ (0.35 g, 0.5 mmol) in hexane (20 mL) methylisocyanide (0.75 mmol) was added at room temperature. The purple color of the solution became yellow, and the reaction mixture was allowed to stir at room temperature overnight, whereupon the color of the solution changed to deep red. All of the volatiles were removed under reduced pressure, and the reddish oil was extracted with ~20 mL pentane and filtered via a filter tip cannula. Free Ge(Ar^{Me₆})₂ and complex 1 were separated from the product by overnight storage of the dilute pentane solution at ca. –18 °C. The mother liquor was decanted from the solids and the volume of the solution was reduced by half and stored at ca. –18 °C overnight to yield deep-red crystals of 1'. Yield: 29% (0.11 g). Mp: 186 °C (red oil). ¹H NMR (600 MHz, C₆D₆, 25 °C): δ 1.85 (3H, br, *p*-Me), 1.89 (3H, s, *N*-Me), 2.21 (6H, s, *o*-Me), 2.31 (6H, br, *o*-Me), 2.37 (3H, s, *p*-Me), 6.58 (1H, br, *m*-Mes), 6.77 (1H, s, *m*-Mes), 6.82 (4H, d, *J*_{HH} = 7.5 Hz, *m*-C₆H₃), 7.02 (1H, t, *J*_{HH} = 7.5 Hz, *p*-C₆H₃), 7.11 (1H, t, *J*_{HH} = 7.5 Hz, *p*-C₆H₃). ¹³C NMR could not be

obtained due to the low solubility of 1'. λ_{max} (ε): 377 nm. IR (ATR) ν(C–N): 1710 cm^{–1} (m).

(Ar^{Me₆})₂GeC(NHMe)C(NMe)C(Ar^{Me₆})NMe (3''). To a stirred slurry of Ge(Ar^{Me₆})₂ (0.35 g, 0.5 mmol) in hexane (20 mL) methylisocyanide (5 mmol) was added at room temperature. The purple color of the solution became yellow, and the reaction mixture was allowed to stir at room temperature for 2 days, whereupon the color of the solution changed to deep red. All of the volatile components were removed under reduced pressure, and the reddish oil was extracted with ~20 mL pentane and filtered via a filter tip cannula. Free Ge(Ar^{Me₆})₂ was separated from the product by overnight storage of the dilute pentane solution at ca. –18 °C. The mother liquor was decanted from the solids, and the volume of the solution was reduced by half. Storage at ca. –18 °C overnight yielded deep red crystals of 3''. Yield: 23% (0.09 g). Mp: 158 °C (dec). ¹H NMR (400 MHz, C₆D₆, 25 °C): δ 1.98 (3H, s, CNMe or Ar^{Me₆}), 2.07 (3H, s, CNMe or Ar^{Me₆}), 2.08 (6H, s, *o*-Me), 2.10, 2.11, 2.13, 2.21, 2.26, 2.34 (all s, 3H, CNMe or Ar^{Me₆}), 4.56 (1H, q, N–H), 6.24 (1H, d, *J*_{HH} = 7.5 Hz, *m*-C₆H₃), 6.59 (2H, br, *m*-Mes), 6.76 (2H, br, *m*-Mes), 6.79 (2H, br, *m*-Mes), 6.88 (2H, d, *J*_{HH} = 7.5 Hz, *m*-C₆H₃), 6.96 (1H, dd, *p*-C₆H₃), 6.98 (2H, d, *J*_{HH} = 7.5 Hz, *m*-C₆H₃), 7.02 (1H, dd, *p*-C₆H₃), 7.16 (2H, m, NCH₂). ¹³C NMR spectrum could not be obtained due to the low solubility of 3''. λ_{max} (ε): 343 nm, 421 nm. IR (ATR) ν(C=C) 639 cm^{–1} (br), ν(C=N) 1729 cm^{–1} (br).

(Ar^{Me₆})₂SnCNMe. Methylisocyanide (5 mmol) was added via a syringe to a stirred solution of Sn(Ar^{Me₆})₂ (0.37 g, 0.5 mmol) in ~20 mL of a 1:1 pentane toluene mixture. The reaction mixture was allowed to stand at ca. –78 °C for 2 weeks, after which time a yellow powder precipitated from the purple solution. The solid was maintained at ca. –78 °C via cooling in a dry ice/acetone bath, while the mother liquor was decanted off and an FTIR spectrum could quickly be obtained before complete dissociation of MeNC and conversion of the yellow powder to a purple solid, which was confirmed to be Sn(Ar^{Me₆})₂ by ¹H NMR spectroscopy; decomp.: ca. –50 °C (free CNMe and Sn(Ar^{Me₆})₂). IR (ATR): ν(C–N) 2197 cm^{–1}.

X-ray Crystallographic Data Collection. Crystals of 1, 1', and 3'' suitable for single crystal X-ray diffraction were removed from a Schlenk flask under a stream of N₂ and immediately covered with a layer of hydrocarbon oil. A single crystal was selected, attached to a glass fiber on a copper pin, and placed in the cold N₂ stream of the diffractometer. Data were collected based upon a single component, processed with SAINT,³⁰ and corrected for Lorentz and polarization effects and absorption using Blessing's method as incorporated into the program SADABS.³¹ The structures were determined by direct methods using the program XS.³² Refinement of the structure was achieved using the program XL.³² All of the nonhydrogen atoms were located initially or from one difference-Fourier map least-squares cycle, and convergence proceeded quickly with all of the hydrogen atoms located from a subsequent difference-Fourier map. See SI for more details.

Details of DFT Calculations. All calculations were done with Turbomole v6.3 program.³³ The geometries of studied systems were optimized with DFT using the hybrid PBE1PBE exchange–correlation functional³⁴ in combination with the TZVP basis sets.³⁵ Due to the size of terphenyl ligands in experimental compounds, calculations were performed for model systems with smaller phenyl substituents. All reported energy values represent reaction enthalpies at 0 K.

In addition to the mechanism discussed in the main text, a number of other pathways were investigated via the calculations. For example, addition of the second equivalent of isocyanide to the germanium prior to phenyl migration resulted in Ge–C bond breaking and simple shuffling of the coordinated isocyanides. If, on the other hand, the second equivalent of methylisocyanide was reacted directly with the carbon in the coordinated isocyanide, coupling of the two isocyanides to a free diamine was observed. Similarly, an attack of the third equivalent of a methylisocyanide to a carbon atom in the azagermacyclobutene intermediate led to a C–C bond formation and to a structure with a three-membered CNN ring with no apparent further reactivity. The possibility of hydrogen transfer occurring before the formation of 3'_{ph} was also tested computationally, but it resulted only in a formation of a five-membered ring with no apparent further reactivity. Hence, the

mechanism discussed in the main text was the only plausible reaction pathway connecting **1** to **3''**_{ph} which could be identified computationally.

RESULTS AND DISCUSSION

Treatment of a purple solution of $\text{Ge}(\text{Ar}^{\text{Me}_6})_2$ with an excess of MeNC immediately yielded a bright yellow solution, indicative of the formation of the adduct species, **1**. Storage of this solution at ca. $-18\text{ }^\circ\text{C}$ yielded X-ray quality yellow crystals of the germylene–isocyanide adduct (see Figure 1 for structural details). The bond

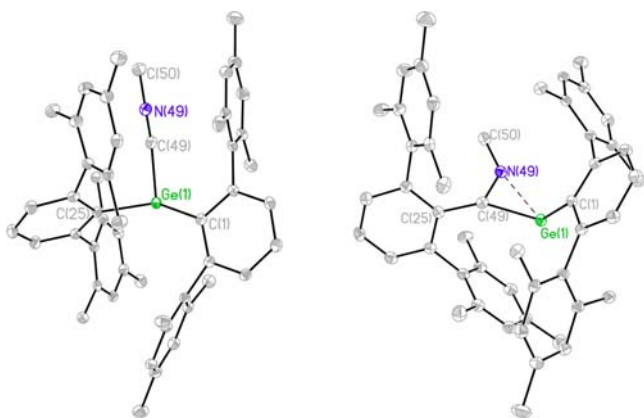


Figure 1. Thermal ellipsoid (30%) drawing of **1** (left) and **1'** (right). Carbon-bound hydrogen atoms and a cocrystallized hexane molecule (in **1'**) are not shown for clarity. Selected bond lengths (Å) and angles ($^\circ$) **1**: Ge(1)–C(1) 2.057(3), Ge(1)–C(25) 2.060(3), Ge(1)–C(49) 2.028(4), C(49)–N(49) 1.164(5), N(49)–C(50) 1.422(5), C(1)–Ge(1)–C(25) 116.6(1), C(Ar)–Ge(1)–C(49) (ave) 96.4(1), Ge(1)–C(49)–N(49) 156.6(3). **1'**: Ge(1)–C(1) 2.046(4), Ge(1)–C(49) 2.021(5), Ge(1)–N(49) 2.104(4), C(49)–C(25) 1.496(4), C(49)–N(49) 1.271(5), N(49)–C(50) 1.465(6), C(1)–Ge(1)–C(49) 107.4(2), Ge(1)–C(49)–N(49) 75.6(3), C(49)–N(49)–C(50) 128.2(4), Ge(1)–N(49)–C(50) 155.2(3), C(25)–C(49)–Ge(1) 150.4(3).

dissociation energy for **1** was found to be -20 kJ mol^{-1} by Van't Hoff analysis of the variable temperature UV–vis spectrum, and it exists in equilibrium with free MeNC and $\text{Ge}(\text{Ar}^{\text{Me}_6})_2$. If the reaction is continued overnight, the yellow solution changes to deep red, and the three-fold insertion product, **3''**, can be isolated in moderate yield ($\sim 25\%$).

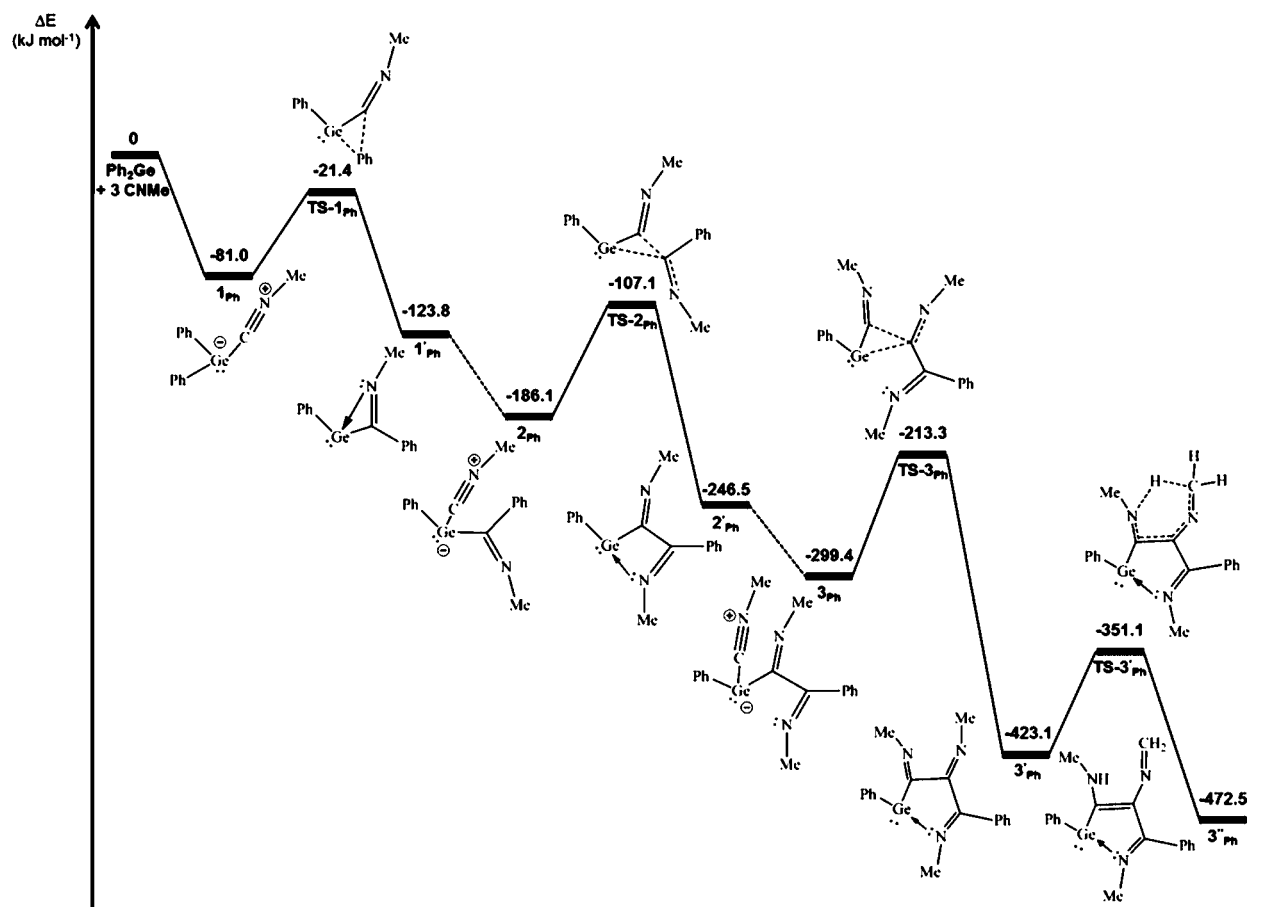
Adduct formation is often an initial step in the reaction of main group species with unsaturated molecules, and synergistic interactions between main group species and the frontier orbitals of the ligand propagate further reaction.³⁶ The infrared spectrum of **1** shows a slight shift of the C–N stretching band to higher frequency (2165 cm^{-1}) in comparison to the free isocyanide (cf. 2161 cm^{-1}), indicative of $n \rightarrow \pi^*$ back-bonding between the germanium(II) lone pair and the π^* orbital of the isocyanide ligand. These data are in good agreement with the spectrum of $(\text{Ar}^{\text{Me}_6})_2\text{GeCNBu}^t$, in which the C–N stretching band is 5 cm^{-1} lower in frequency.²⁷ In contrast, the tin congener of **1**, $(\text{Ar}^{\text{Me}_6})_2\text{SnCNMe}$, can only be isolated at low temperatures with use of a 10-fold excess of MeNC and readily dissociates to $\text{Sn}(\text{Ar}^{\text{Me}_6})_2$ and MeNC above ca. $-50\text{ }^\circ\text{C}$. Although the bonding between MeNC and $\text{Sn}(\text{Ar}^{\text{Me}_6})_2$ is weak, the C–N stretching band in the infrared spectrum of $(\text{Ar}^{\text{Me}_6})_2\text{SnCNMe}$ is shifted by 36 cm^{-1} to higher frequency. The direct comparison between isoleptic tetrelene–isocyanide adducts does not support the view that hypsochromic shift of the C–N stretching band is directly

proportional to the M–C bond strength but that the back-bonding interaction in complex **1** plays a large role in the strength of the dative bond.³⁷

To suppress the subsequent isocyanide insertions which lead to the formation of **3''**, only 1.5 equiv of MeNC was added to a solution of the germylene to produce the one-fold insertion product, **1'**. X-ray quality red crystals of **1'** (structure, Figure 1) had a Ge(1)–C(1) bond length of 2.046(4) Å, which is very close to that in $\text{Ge}(\text{Ar}^{\text{Me}_6})_2$ (cf. 2.033(4) Å). The Ge(1)–C(49) bond length of 2.022(5) Å is also very similar to that of the Ge–C(1) bond. The C(1)–Ge(1)–C(49) bond angle of $107.4(2)^\circ$ is less than that ($114.4(2)^\circ$) in $\text{Ge}(\text{Ar}^{\text{Me}_6})_2$.²⁸ The C(49)–N(49) bond length of 1.271(5) Å in the isocyanide indicates the conversion of the triple bond to a double bond, and the lowering of the bond order is confirmed by a decrease in the C–N stretching frequency to 1710 cm^{-1} in comparison to the 2165 cm^{-1} in **1**. Additionally, the nitrogen lone pair is now datively bound to the germanium through the p-orbital of the germylene. The Ge(1)–N(49) distance (2.104(4) Å) is long,³⁸ and the dative bond creates an acute Ge(1)–C(49)–N(49) angle of $75.6(3)^\circ$ at C(49). These two factors, coupled with a broadened ^1H NMR spectrum for **1'** are indicative of a relatively weak Ge–N bond that is dissociating in solution. Overall, the structural and spectroscopic data do not strongly support a side-on, π -bonded model for the CN double bond of the $\text{Ar}^{\text{Mes}}_6\text{CNMe}$ unit with Ge(1).

In order to understand the initial migratory insertion of MeNC into the Ge(1)–C(Ar) bond, we examined the possible reaction pathway (Scheme 3) for the formation of **3''** by use of DFT (see Supporting Information, SI) and via the isolation of the intermediates **1** and **1'** and the product **3''**. The model complex, $\text{Ge}(\text{C}_6\text{H}_5)_2$, was used to study the reaction pathway computationally. Although the replacement of bulky terphenyl groups with the significantly smaller phenyls will certainly have some effect on the calculated energies, it is unlikely to have a major effect on the mechanism, especially in view of the relatively small size of CNMe. The formation of the model adduct species **1_{ph}** was found to be more stable than the free starting materials. A transition state (TS-**1_{ph}**) was found for the formation of **1'_{ph}** which involves the concerted migration of the isocyanide molecule into the Ge–C(Ph) bond. We hypothesize that the insertion reaction depends on having a highly activated, electron-rich germanium atom, and removal of this electron density is accomplished by either dissociating to the free starting materials or migratory insertion of the isocyanide molecule. The activation energy for this process is predicted to be less than the energy gained from the dative bond formation, and the coordination number at the germanium is maintained through a weak dative interaction with the β -nitrogen of the imino moiety.

As mentioned earlier, the N–Ge dative bond in **1'** is relatively weak, and in the presence of excess isocyanide, it is readily broken and is replaced by a second isocyanide molecule which possesses a greater electron-donating capability than the imino-nitrogen. The second adduct species, **2_{ph}**, undergoes a further migratory insertion process (TS-**2_{ph}**) in a manner similar to the first insertion, yielding an azagermacyclobutene complex **2'_{ph}** which, like **1'_{ph}**, possesses a dative interaction between the γ -nitrogen and germanium. As before, formation of an isocyanide adduct complex of **2'_{ph}** is energetically favored and is rapidly followed by a third migration of MeNC to yield the heterocyclic complex **3'_{ph}**. The C–H bond activated complex, **3''_{ph}**, is predicted to be more stable than **3'_{ph}** by 49 kJ mol^{-1} and adopts a cyclopentadienyl-type structure after hydrogen transfer.

Scheme 3. Calculated Reaction Pathway for the formation 3''_{ph}

The final product 3''_{ph} is predicted to be favored over the tris-imino complex 3'_{ph} for steric reasons. We hypothesize that there is considerable steric strain placed on the α and β imine bonds by the aryl ligands, and the bond reduction allows these bonds to bend inward away from the bulky aryl ligands. Relief of this bond strain, coupled with the energy gained by allowing the C–N bond to freely rotate away from the germanium-bound ligands, is sufficient to overcome the calculated activation energy of 72 kJ mol⁻¹.

Deep-red crystals of 3'' suitable for X-ray diffraction were isolated from a concentrated pentane solution, and the structure is shown in Figure 2. The diene fragment comprised of N(49)–C(49)–C(51)–C(53) is twisted 13.7(4)° from planarity, and the sum of angles within the five membered ring is 560.5°. The C(51)–N(51) and C(53)–N(53) bond lengths are 1.413(3) and 1.345(5) Å, and the contracted distance of the sp²–sp³ C(53)–N(53) bond is indicative of conjugation between the nitrogen lone pair and the unsaturated heterocycle. The conjugation is further supported by broadening of the ¹H NMR spectrum for the amido and alkenyl protons. The C(49)–N(49) bond (1.333(3) Å) maintains its imido character, and the Ge(1)–N(49) (1.968(2)) is short for germanium bound dative bonds (cf. 2.104(4) Å in 1'). We attribute the increased strength of the germanium–nitrogen dative bond to a decrease in the steric bulk at the germanium atom as well as ability for the γ isocyanide fragment to freely coordinate without causing undue bond strain as in 1'. Migratory insertion reactions have been reported by our group for the reaction of CO with germylenes, although no CO adduct analogues of 1' could be isolated.³⁹ Driess and co-workers have also reported coupling reactions for isocyanides with silylenes

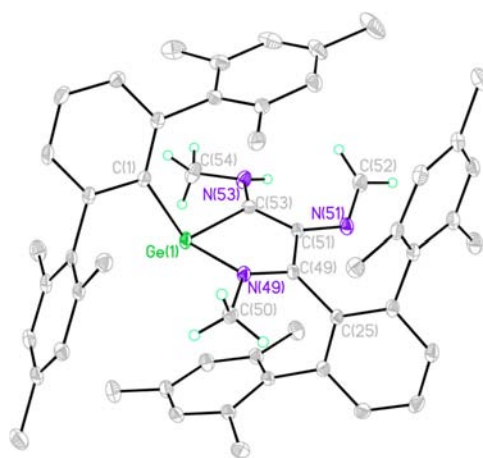


Figure 2. Thermal ellipsoid (30%) drawing of 3''. Carbon-bound hydrogen atoms of the *m*-terphenyl ligands are not shown for clarity. Selected bond lengths (Å) and angles (°): Ge(1)–C(1) 2.036(3), Ge(1)–C(53) 1.992(3), Ge(1)–N(49) 1.968(2), C(49)–N(49) 1.333(3), N(49)–C(50) 1.455(3), C(25)–C(49) 1.510(3), C(49)–C(51) 1.423(4), C(51)–N(51) 1.413(3), N(51)–C(52) 1.265(4), C(51)–C(53) 1.401(4), C(53)–N(53) 1.345(4), N(53)–C(54) 1.460(4), C(1)–Ge(1)–C(53) 107.9(1), C(1)–Ge(1)–N(49) 108.5(1), Ge(1)–N(49)–C(49) 111.4(2), Ge(1)–C(53)–C(51) 110.2(2), C(51)–N(51)–C(52) 120.1(3), C(49)–N(49)–C(50) 123.8(2).

stabilized by β -diketiminato ligands, but at present, no mechanistic information is available for these reactions.⁴⁰

CONCLUSION

In conclusion, we have prepared an azagermacyclopentadienyl species by the three-fold insertion of methylisocyanide into the germanium–carbon bond of a diarylgermylene. Additionally, we have isolated key intermediates in this reaction which, along with DFT calculations, have provided further insight for the coupling reactions of unsaturated organic molecules with heavy carbene analogues. Further study of coupling reactions between **1** and other substrates is underway as well as investigations into catalytic capabilities of the migratory insertion reactions.

ASSOCIATED CONTENT

Supporting Information

Crystallographic information files for **1**, **1'**, and **3''**; ^1H NMR spectra for **1'** and **3'**; temperature-dependent UV–vis spectra for **1**; tables of crystallographic data and collection parameters for **1**, **1'**, and **3''**. Computational details for **1_{Ph}**, **1'_{Ph}**, **2_{Ph}**, **TS-2_{Ph}**, **2'_{Ph}**, **3_{Ph}**, **TS-3'_{Ph}**, and **3''_{Ph}**. This material is available free of charge via the Internet at <http://pubs.acs.org>.

AUTHOR INFORMATION

Corresponding Author

pppower@ucdavis.edu; heikki.m.tuononen@jyu.fi

Notes

The authors declare no competing financial interest.

ACKNOWLEDGMENTS

We thank the U.S. Department of Energy (DE-FG02-07ER46475), the Academy of Finland and the Technology Industries of Finland Centennial Foundation for funding.

REFERENCES

- (1) Suginome, M.; Ito, Y. *Adv. Polym. Sci.* **2004**, *171*, 77–136.
- (2) Marcilly, C. *J. Catal.* **2003**, *216*, 47–62.
- (3) Malpass, D. *Introduction to Industrial Polyethylene*; Wiley-Scrivener: Hoboken/Salem, 2010.
- (4) Millich, F. *Macromol. Rev.* **1980**, *15*, 207–253.
- (5) Frühauf, H.-W. *Chem. Rev.* **1997**, *97*, 523–596.
- (6) Passerini, M.; Ragni, G. *Gazz. Chim. Ital.* **1931**, *61*, 964–969.
- (7) Dömling, A.; Ugi, I. *Angew. Chem., Int. Ed.* **2000**, *112*, 3300–3344.
- (8) Ugi, I. *Angew. Chem., Int. Ed.* **1962**, *1*, 8–21.
- (9) Ugi, I.; Steinbrückner, C. *Chem. Ber.* **1961**, *94*, 734–742.
- (10) Denmark, S. E.; Fan, Y. *J. Org. Chem.* **2005**, *70*, 9667–9676.
- (11) Biggs-Houck, J. E.; Younai, A.; Shaw, J. T. *Curr. Opin. Chem. Biol.* **2010**, *14*, 371–386.
- (12) Lygin, A. V.; de Meijere, A. *Angew. Chem., Int. Ed.* **2010**, *49*, 9094–9124.
- (13) Ugi, I.; Fetzer, U. *Chem. Ber.* **1961**, *94*, 2239–2243.
- (14) Yamamoto, Y.; Hagihara, N. *Nippon Kagaku Zasshi* **1968**, *89*, 898–900.
- (15) Stackman, R. W. *J. Macromol. Sci. Chem.* **1968**, *A2*, 225–236.
- (16) Yamamoto, Y.; Takizawa, T.; Hagihara, N. *Nippon Kagaku Zasshi* **1966**, *87*, 1355–1359.
- (17) Kamer, P. C. J.; Nolte, R. J. M.; Drenth, W.; Nijs, H. L. L. M.; Kanters, J. A. *J. Mol. Catal.* **1988**, *49*, 21–32.
- (18) Walborsky, H. M.; Morrison, W. H.; Niznik, G. E. *J. Am. Chem. Soc.* **1970**, *92*, 6675–6676.
- (19) Hitchcock, P. B.; Lappert, M. F.; Layh, M. *Angew. Chem., Int. Ed.* **1999**, *38*, 501–504.
- (20) Hitchcock, P. B.; Lappert, M. F.; Layh, M. *Chem. Commun.* **1998**, 201–202.
- (21) Li, X.; Ni, C.; Song, H.; Cui, C. *Chem. Commun.* **2006**, 1763–1765.
- (22) Cook, K. S.; Piers, W. E.; Hayes, P. G.; Parvez, M. *Organometallics* **2002**, *21*, 2422–2425.

(23) MacMillan, S. N.; Tanski, J. M.; Waterman, R. *Chem. Commun.* **2007**, 4172–4174.

(24) Porchia, M.; Ossola, F.; Rossetto, G.; Zanella, P.; Brianese, N. *J. Chem. Soc. Chem. Commun.* **1987**, 550–551.

(25) Uhl, W.; Schütz, U.; Hiller, W.; Heckel, M. *Chem. Ber.* **1994**, *127*, 1587–1592.

(26) Uhl, W.; Hahn, I.; Schütz, U.; Pohl, S.; Saak, W.; Martens, J.; Manikowski, J. *Chem. Ber.* **1996**, *129*, 897–901.

(27) Brown, Z. D.; Vasko, P.; Fettingner, J. C.; Tuononen, H. M.; Power, P. P. *J. Am. Chem. Soc.* **2012**, *134*, 4045–4048.

(28) Simons, R. S.; Pu, L.; Olmstead, M. M.; Power, P. P. *Organometallics* **1997**, *16*, 1920–1925.

(29) Schuster, R. E.; Scott, J. E.; Casanova, J. *Organic Syntheses* **1973**, 772–774.

(30) Blessing, R. H. *Acta Crystallogr.* **1995**, *A51*, 33–38.

(31) Sheldrick, G. M. *SADABS (Siemens Area Detector Absorption Correction)*, version 2008/3; Universität Göttingen: Göttingen, Germany.

(32) Sheldrick, G. M. *SHELXS97 and SHELXL97*; Universität Göttingen: Göttingen, Germany, 1997.

(33) *TURBOMOLE*, v6.3; University of Karlsruhe and Forschungszentrum Karlsruhe GmbH: Karlsruhe, Germany, 2011; <http://www.turbomole.com>.

(34) (a) Perdew, J. P.; Burke, K.; Ernzerhof, M. *Phys. Rev. Lett.* **1996**, *77*, 3865–3868. (b) Perdew, J. P.; Burke, K.; Ernzerhof, M. *Phys. Rev. Lett.* **1997**, *78*, 1396. (c) Perdew, J. P.; Ernzerhof, M.; Burke, K. *J. Chem. Phys.* **1996**, *105*, 9982–9985. (d) Adamo, C.; Barone, V. *J. Chem. Phys.* **1999**, *110*, 6158–6170.

(35) Schäfer, A.; Huber, C.; Ahlrichs, R. *J. Chem. Phys.* **1994**, *100*, 5829–5835.

(36) Li, J.; Hermann, M.; Frenking, G.; Jones, C. *Angew. Chem., Int. Ed.* **2012**, *51*, 8611–8614.

(37) For further discussion, see: Nakamoto, K. *Infrared and Raman Spectra of Inorganic and Coordination Compounds*, 4th ed.; Wiley: New York, 1986.

(38) cf. 1.968(2) Å in the structure of **3''** and $\text{ge-N} = 1.876(5)$ Å in the $\text{Ge}\{\text{N}(\text{SiMe}_3)_2\}_2$; Chorley, R. W.; Hitchcock, P. B.; Lappert, M. F.; Leung, W.-P.; Power, P. P.; Olmstead, M. M. *Inorg. Chim. Acta.* **1992**, *188-200*, 203–209.

(39) Wang, X. P.; Zhu, Z. L.; Peng, Y.; Lei, H.; Fettingner, J. C.; Power, P. P. *J. Am. Chem. Soc.* **2009**, *131*, 6912–6913.

(40) Xiong, Y.; Yao, S.; Driess, M. *Chem.—Eur. J.* **2009**, *15*, 8542–8547.